A Miniaturised Space Qualified MEMS IMU for Rover Navigation
Requirements and Testing of a Proof of Concept Hardware Demonstrator

Felix Rehrmann[(1)], Jakob Schwendner[(1)], John Cornforth[(2)], Dick Durrant[(2)], Robert Lindegren[(3)], Per Selin[(3)], Javier Hidalgo Carrio[(4)], Pantelis Poulakis[(4)], Johan Köhler [(5)]

[(1)]DFKI GmbH, Robotics Innovation Center, Robert-Hooke-Straße 5, 28359 Bremen, Germany, Email: Felix.Rehrmann@dfki.de, Jakob.Schwendner@dfki.de

[(2)]SEA, Building 660, Bristol Business Park, Coldharbour Lane, Bristol, BS16 1EJ, United Kingdom, Email: John.Cornforth@sea.co.uk, Dick.Durrant@sea.co.uk

[(3)]ÅAC MicrotecAB, Uppsala Science Park, SE-751 83 Uppsala, Sweden, Email: Robert.Lindegren@aacmicrotec.com, Per.Selin@aacmicrotec.com

[(4)] Automation and Robotics Section, ESTEC, European Space Agency, Noordwijk, The Netherlands, Email: havyhidalgo@gmail.com, Pantelis.Poulakis@esa.int

[(5)]Swedish National Space Board, Solna, Sweden, Email: Johan.Kohler@snsb.se

ABSTRACT

A recent ESA R&D activity, led by ÅAC, including SEA and DFKI, was undertaken to develop a miniaturised MEMS based inertial measurement unit (IMU) for use in rover navigation systems for planetary or lunar exploration missions. It has been part of the Technology Research Program (TRP) at ESTEC allocated in the Automation & Robot Section. The miniaturised IMU study showed the feasibility of such a unit by deriving requirements from the targeted missions, and showing how these can be met. The study was supported by developing, manufacturing and testing a functional breadboard demonstrator and by testing material mock-ups under target environmental conditions. This paper provides a brief introduction into the design options, the miniaturisation using ÅAC proprietary multi wafer packaging 'via' technology and the results of the environmental tests. Another focus lies on the derivation of the requirements, and the testing of the IMU breadboard prototype.

1 INTRODUCTION

Autonomous navigation of rovers in extraterrestrial exploration is highly influencing the mission's success chances. The navigation directly depends on the sensory data which enable the rover to localize itself within its environment. The need to localize itself with certain accuracy while performing the navigation task in a harsh and remote environment makes the design of the navigation system a trade off between sensor performance and cost in power, weight and mass. Using the improving MEMS technology and advanced packing technologies looks like a promising way to develop a unit that delivers valuable data to the navigation system while using relatively little space, mass and volume of the system.

As stated in the statement of work (SOW) [1] the objective of the presented activity was to design and demonstrate an IMU that can be used for navigation in the context of rover-based exploration missions on Moon or Mars. Table 1 lists the base specifications.

Table 1. Base specifications from [1].

Requirements from Statement of Work
Support localisation on planetary terrain with an accuracy of better than 2% over a representative trajectory.
CAN Interface (acc. ECSS-E-50-09, sec. 5)
Power Interface (acc. ECSS-E-20A, sec. 5.6 and 5.7)
Mars & Lunar Surface Operation
Tolerant to Radiation occurring at transfer and operation
Survive unpowered in -135°C to 70°C with 0 to 7 mbar and on earth (1bar).
Mass < 200 g and power consumption < 1 W.
Provide real-time data when powered. 3-axis rates and accelerations, sensor temperatures and housekeeping data.

The solution for the given task is materialising in several steps. It starts with refining the requirements, which is described in chapter two. An overview about the architecture considerations to realise the hardware and about the breadboard design to show the functional feasibility is given in chapter three. Chapter four points

on the miniaturisation technique and testing, and shows that it is possible to have a small but space qualified unit. The fifth chapter focuses on the breadboard testing. Finally in the sixth chapter the work is summarised with a look into what could be next.

2 REQUIREMENTS

2.1 General

The requirements are subdivided into system requirements (related to functional and performance properties), interface requirements and environmental requirements. The system has to survive and operate in a harsh environment - not only on the extraterrestrial body but also during launch and transfer. Furthermore there are requirements to be able to properly operate the IMU within the navigation system and on the rover. This is related to interfaces, operation durations and start-up time. The ExoMars mission for example, requires a lifetime of 180 sols and due to the extreme temperature differences between day and night the IMU will be switched off for some time. After switch-on, the IMU shall be able to provide useful data after a specified time limit. The representative radiation environment has been derived from [4] for a six month period. This yielded the summary radiation-related requirements:

- The shielding shall be equal or greater than 2.5 mm aluminium,
- The components must withstand a total dose of 10 krad
- The system must not be disturbed by a SEE of < 37 MeV cm^2/mg
- The system shall resume operation after a SEE of < 75 MeV cm^2/mg

2.2 Mission and Rover Navigation

Inertial navigation approaches use data from inertial sensors - rate and acceleration sensors - to do dead reckoning of orientation and/or position. Due to the typical errors in the sensors and integration of the sensor readings the navigation cannot solely depend on this kind of information. Inertial navigation is complementary to or integrated with sensors that provide absolute information. Furthermore, the IMU can be used to detect slipping and sliding or other abnormal situations, like collisions.

To breakdown the overall accuracy requirement the typical rover mission scenarios have been investigated and sensor accuracy requirements have been derived. For example, the NEXT-LL scenario [3] gives tasks like analysis of soil samples at regular intervals (100m), service of seismometer payloads (SRS) that will operate on the moon for long period of time (more than six months) and Service of the Lunar Radio-Astronomy Explorer (LRX).

Of course there are other tasks imaginable but all have in common that a given distance/path must be covered with knowing one's position up to certain accuracy in the end. In the requirements the following scenarios have been identified:

- The navigation subsystem should be able to reach a specified location with great accuracy (below 1m).
- 5m of error over 100m of travel would allow for longer autonomous cycles.
- Localise the rover over long ranges (at least one kilometer). An acceptable localisation error in this context is 0.1%: 1m of error for 1km of travel.
- Returning to base scenarios: Depending on the travelled distance the error is estimated to be from 10% to 1% of this distance, assuming that the rover can see its base from at least a 100m.

Figure 1 depicts a generic navigation cycle. It consists of three basic systems. An IMU/odometer system would continuously sum up rates and speed to calculate the travelled distance. The visual odometer would compare two pictures taken at two different times to determine the motion which has been done between them. A SLAM algorithm which uses landmarks to get a global position measurement is done every 10m to 100m. Instead of SLAM other types of global position measurements could be used like a sun sensor, a star tracker or maybe in some distant future even some sort of extraterrestrial GPS.

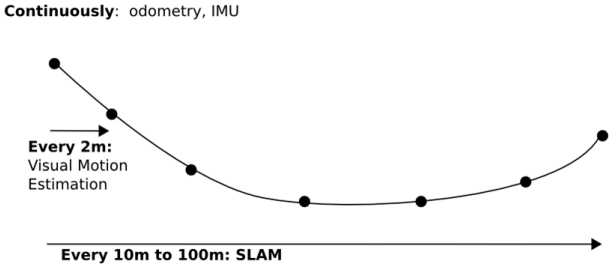

Figure 1. Generic rover navigation cycle.

The IMU built in this project should allow removing the visual motion estimation step altogether. Moreover, in pure point-to-point navigation scenarios, where precise long-range localisation is not required, it should allow navigations up to 100m. The accuracy requirements are based on these constraints.

2.3 Navigation Requirements

To derive the requirements for the sensors and the post processing from the stated mission scenarios a simulation was performed, which determines the error

for a 100 m travel using an IMU in combination with an odometer. The main error of the rate sensors are the angular random walk (ARW) and the bias stability (BS). Both errors are contributing to the drift in the orientation. The acceleration sensors are used to determine the gravity's direction and are presented by a single angle error (Eacc). Since the gravity vector is an absolute measurement, it can bound the integrated orientation error related to the horizontal plane. The odometer is assumed to have an error of 3%. Several simulations have been done with different sensor error values. Table 2 shows the allowed errors to achieve an accuracy of 5% in position after the 100m travel.

Table 2. Acceptable errors to meet the desired accuracy.

Speed (m/s)	ARW (deg/sqrt(h))	BS (deg/h)	Eacc (millig)
0.01	< 0.5	< 1	< 1.5
0.04	< 0.5	< 5	< 1.2
		< 4	< 1.5
0.07	< 0.5	< 9	< 1.5
> 0.1	< 0.5	< 10	< 1.5

The results show that the requirements are relaxed for faster rovers. The sensor requirements are summarized in Table 3.

Table 3. Requirements on the sensors.

Feature	Value
Gyro Dynamic Range	± 24 deg/s
Gyro In-Run Bias Stability	5 deg/h
Angular Random Walk	0.5 deg/sqrt(h)
Accelerometer In-Run Bias Stability	1.2 millig

3 THE UNIT

3.1 System Architecture

Architectural design of the system suggests the IMU system to be built up by three perpendicular sensor units (each unit consisting of one gyro and one accelerometer), one sensor control unit, an optional core unit and a power supply unit. The system function was demonstrated on the breadboard IMU with expected results, giving evidence that a miniaturised IMU with the developed architecture and the targeted sensors is feasible and would give benefit to a rover navigation platform. Such an IMU would provide important data for short distance dead reckoning navigation with low costs in power, weight and size.

Four different alternatives for an IMU concept were proposed, ranging from a version using packaged, commercial components to a fully miniaturized version utilizing bare die components, interposers and ceramic MCMs (Multi-Chip Module) with flip-chipped bare dies. An overview of the properties of the alternatives can be seen in Table 4:

Alt.1: Packaged components in standard packages.
Alt.2: Mix between the MCM technology and components in normal packages.
Alt.3: As Alt.2 but with sensor front-end electronics embedded in mixed signal ASICs.
Alt4: Highest packed solution, including the mixed signal ASIC design from Alt.3.

Table 4. Estimated properties of design alternatives.

Properties	Alt. 1	Alt. 2	Alt. 3	Alt. 4
Volume [cm³]	1000	545	291	180
Weight [g]	450	245	185	143
Req. Work 0-None / 5-most	1	3	4	5

Except for alternative 1, all approaches need some further development regarding packaging and components. But the benefit would be a substantial reduction of volume and mass. The best trade-off between effort and benefit would be alternative 2. All four designs use a flex-rigid solution where three PCB boards are folded in three perpendicular axes for attaining desired function and also to gain easy contacting between the boards, as illustrated in Figure 2. The flex can pass the signals between the rigid PCB boards without adding extra connectors and wiring between the boards. The alternative to integrate three perpendicular LTCC (Low Temperature Co-fired Ceramic) substrates would add both extra contacting issues and additional complexity in the assembly and calibration phase.

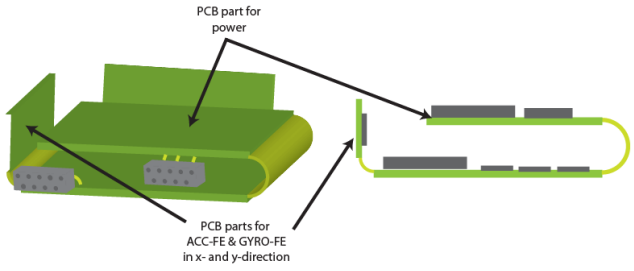

Figure 2. Module Package Design

During the concept design several critical items were identified and addressed. On the packaging side one drawback for polymer carrier boards is the poor temperature behavior due to the relatively high CTE value (Coefficient of Thermal Expansion) which makes the thermal reliability for components soldered directly

to the board low. In order to avoid bare dies being attached directly to PCB the miniaturized concepts propose the use of silicon interposers and LTCC MCM which can increase the tolerance to thermal stress in the solder interfaces.

3.2 Breadboard

The IMU breadboard concept demonstrator was designed using existing modules from SEA, DFKI and a newly designed accelerometer module. The assembled unit is supplied from a 28Vdc power input with telemetry data transmitted over a CAN interface. The breadboard IMU includes the architectural system interfaces necessary for commissioning and testing both the individual modules and the complete IMU, including the necessary gyro and accelerometer sensors. It was manufactured to be a robust, reliable unit which could be mounted on various mechanical interfaces.

One high performance harmonised space grade gyro sensor was used for the yaw axis with lower grade commercial gyro sensors in the pitch and roll axis due to study cost constraints. At present there is no European space-qualified MEMS accelerometer although there is a current ESA study to develop one, led by SEA. A commercial high-performance accelerometer from Colibrys was chosen as a substitute. On the breadboard, the CAN interface and all sensor information is integrated on a commercial microcontroller. For the qualified unit, this task would be handled in an FPGA.

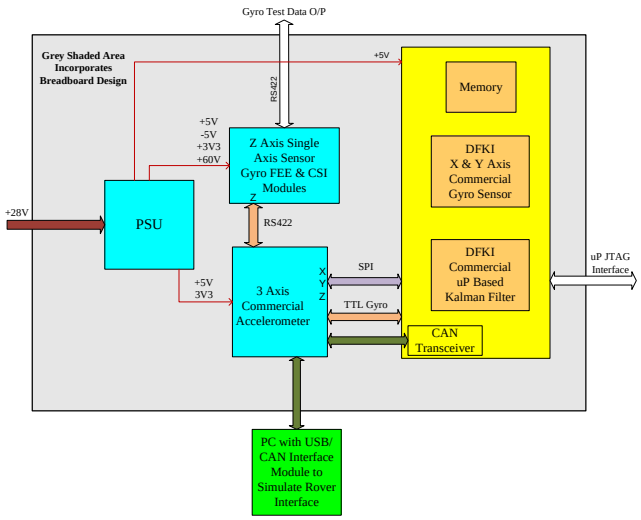

Figure 3. Architecture of Breadboard IMU

Figure 3 illustrates the Architecture Design and integration of the modules that make up the Breadboard IMU.

The concept hardware breadboard IMU comprises the following integrated modules:

- Harmonized Single axis SEA Gyro Module (consisting of an AIS MEMS Gyro Sensor, front-end electronics module, PSU and a CSI module), Front-End Electronics module, Power Supply Unit and a Control & Spacecraft Interface module.
- A DFKI dual axis commercial Gyro module (consisting of commercial gyro's and a commercial uP with a software Kalman Filter) including a CAN interface.
- A triple axis commercial Accelerometer module (consisting of 3 single axis +/- 10g Colibrys MS9000.D capacitive accelerometers, signal conditioning and a 12bit ADC). This module also includes the connectivity and electronics to allow interfacing between the SEA MRS Gyro modules, the DFKI IMU module using SPI and RS422 and the external CAN/Power connectors.

The breadboard IMU delivers data to the rover's data handling system (DHS) in the Rover over a CAN bus. The DHS collects the CAN stream and converts the bytes into the values, as they are measured and processed by the IMU. For the testing, all data existed as raw telemetry values as well as in the format of CAN message log files to get orientation of the IMU with respect to a global frame of reference.

For the breadboard the post-processed data was used, as this allowed testing of the Kalman filter in an integrated environment. In addition, housekeeping data and commands can be sent/received over the CAN bus. A synchronization pulse (PPS) is also provided for as an option if required from the rover DHS. The completed manufactured breadboard IMU is shown in Figure 4 below.

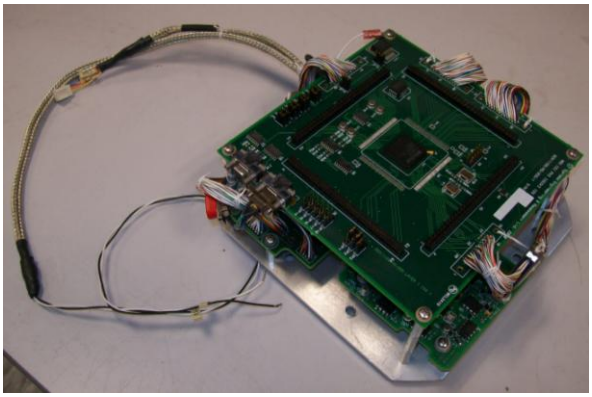

Figure 4. Concept Breadboard IMU Demonstrator

4 MINIATURISATION AND MATERIAL TESTS

Both silicon and LTCC substrates are used when electronic circuits, passive components and sensors are surface mounted or integrated to the substrate. Due to the requirements in size and hermeticity, it is necessary

to design the integrated system with several substrates mounted on top of each other. In order to achieve electrical contact between each substrate level, electrical through substrate vias are needed. ÅAC has developed an electrical through silicon wafer via which both provides a very high manufacturing yield and is compatible with standard MEMS processing. This has been investigated by testing structural mock-ups, which model the main failure modes.

Common LTCC substrates can be ordered directly from the substrate manufacturers with through substrate vias. The electrical connection between the substrates is then ensured using BGA interface. The following items were identified critical in regard to future miniaturization:

- BGA solder joint reliability between ceramic/silicon modules and PCB carrier board
- Gyro and accelerometer mounting and naked die preparation for flip-chip
- The failure mechanism of internal routing cracking in LTCC
- The failure mechanism of through silicon vias cracking in Si interposers
- Parylene™ coating reliability
- Break-down voltage between BGA I/O's

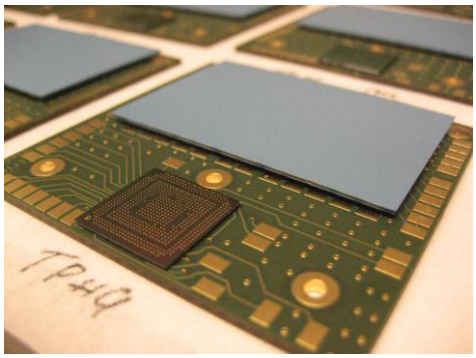

Figure 5. Structural testing mock-up modules

The sensor mounting and the break-down voltage could be mitigated by analysis. The remaining issues have been regarded in the material tests. Structural mock-ups (see Figure 5) representing relevant hardware have been tested against the following environmental influences:

- Thermal cycling survival -135°C to 85°C,
- Thermal cycling operation -55°C to +80°C,
- Vibrations XYZ-direction (sinus, random),
- Shock (1500g) and
- Vacuum (0 to 1 bar).

The temperature cycling tests showed as expected that it is important to precisely match the required coefficient of thermal expansion (CTE). Given that materials are properly chosen, the tests and additional analysis have proven that the proposed packaging solution is feasible and robust for a miniaturized IMU concept.

5 BREADBOARD TESTING

The breadboard tests were conducted with regard to the functionality in general as well as in regard to the usability in a rover application.

5.1 Test Setups

Initial integration checks were undertaken to functionally test the complete system before the overall unit calibration was carried out. Calibration of the sensors was carried out using a rate table at SEA and by rotating the unit through the gravity field. Then the unit was mounted on a robotic arm at DFKI (see Figure 6), to generate specific trajectories, used on a DFKI high dynamic mobile robot [9] with a low signal to noise ratio and on the LRM ESA Rover [6] which represents a target application system.

Figure 6. Impressions from the demonstrator tests. Left: IMU breadboard on DFKI robotic arm. Right: IMU breadboard on ESA LRM rover.

Additionally the system noise characterisation has been performed with the Allan Variance method. The Allan Variance [5] is a statistical tool to characterise the stability and quality of a time and frequency system over cluster time. The inertial sensor community has adopted it as part of the IEEE standard recommendation for testing inertial sensors [7], [8]. Data were collected at room temperature in the Metrology laboratory of ESTEC [6] on an anti-vibration table for around eight hours at 55Hz.

Selected results from the tests are presented. During the tests the data sent over the CAN bus were collected. This is raw data (byte values without physical unit) for the 3 axes; each has a rate, acceleration and two temperatures, one for each sensor. The raw data of the SEA rate sensor already includes compensation of secondary effects. Additionally the reference data has been recorded. The reference for the robotic arm is the joint angles of the 7 directions of freedom Mitsubishi

PA10 arm. For the mobile systems tests, the outdoor reference is a differential global positioning system (DGPS) while indoors the system is tracked with a VICON motion capture system.

The collected data were processed. This post-processing included the transformation of the raw byte values to the floating point values which have a physical unit. The evaluation processing steps differ depending on the subject of interest.

5.2 Breadboard Test Results

The SEA Gyro was calibrated on a rate table for a range of ±24°/s rate in one degree steps and the resulting error graph is illustrated in Figure 7. Rate Bias temperature compensation was also undertaken giving temperature movements over a 40°C range of approx.10deg/hr.

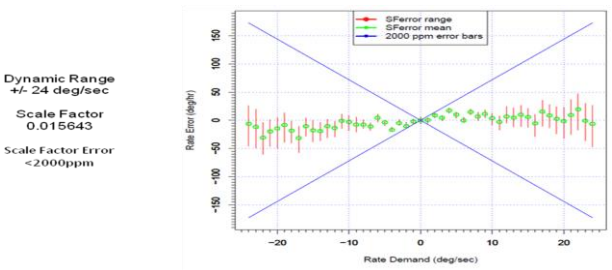

Figure 7. SEA Gyro Rate Error Plot

The result of applying the Allan variance technique to the SEA gyro can be seen in Figure 8. The curve fits a straight line of slope -1/2 for short cluster times (τ). This is characteristic of angle random walk and the noise coefficient is obtained by reading the slope line at $t = 1$. Figure 8 also shows a line of +1/2 slope for the long cluster times. This is representative of a rate random walk noise and the coefficient can be obtained by reading the slope line at $t = 3$. The central part of the curve is characteristic of a zero slope. The lowest point on the curve gives the bias instability coefficient, which represents the best stability of the run. The values are summarized in Table 5.

Table 5. Dominant noise coefficients for SEA gyro.

	ARW	BS	Rate random walk
SEA gyro	0.018 °/sqrt(h)	1°/h	5 °/h/sqrt(h)

Similar analysis has been done for the accelerometers. The Allan variance graph (Figure 9) shows that the velocity random walk is the dominant error for short cluster time, which curve fits a straight line of -1/2 slope and the numerical value is also obtained by reading the slope line at $\tau=1$.

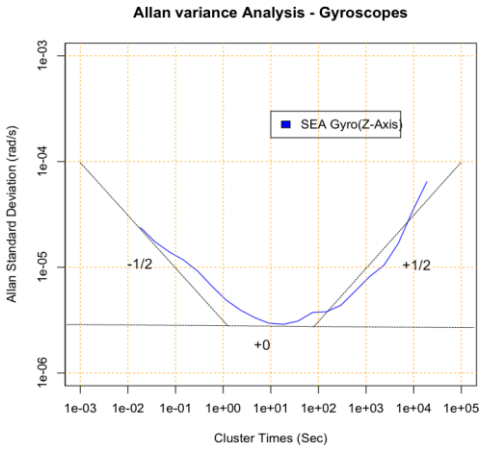

Figure 8. Allan variance analysis for SEA gyro.

The bias instability of the accelerometers is also representative of a zero slope in the central part of the curve. Longer recorded data from accelerometers would be needed to better identify the kind of stochastic error underlying the last part of the curve, which does not have any clear slope. An estimation of an acceleration random walk can be deduced from the x-axis where the plot more clearly describes a +1/2 slope. The resulting properties are listed in Table 6.

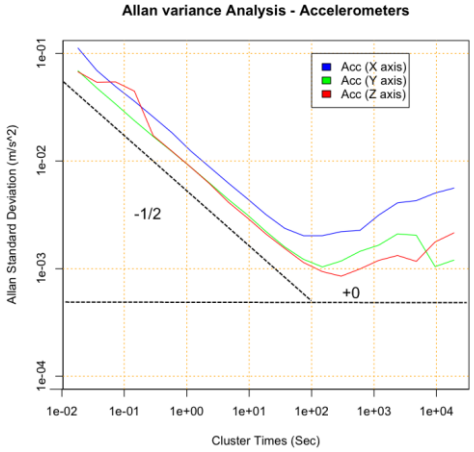

Figure 9. Allan variance analysis for accelerometers.

Table 6. Dominant noise coeff. for Accelerometers.

	Velocity random walk [m/s/sqrt(h)]	Bias instability [m/s^2]	Acceleration random walk [m/s^2/sqrt(h)]
X-axis	0.84036	0.003045	0.00948
Y-axis	0.58309	0.001562	0.00617
Z-axis	0.58431	0.001280	0.00360

The first test performed to check the calibration of the breadboard and to get first results for the accuracy is a robotic arm test with the end effector describing a half sphere to obtain orientations covering a wide subset of all possible orientations. The resulting data has been processed in two ways. The accelerometers' accuracy is analysed by comparing the g-Vectors measured by the IMU with that one obtained from the robotic arm pose. Table 7 shows the results from the accelerometer analysis. It can be seen that the accelerometers are better than expected.

Table 7. Accelerometer errors from robotic arm test.

Error Type	Required	Expected	Results
Accel. Error [millig]	1.2	75	9.84
Horiz. Plane Err. [°]	not given	6.54	1.41

The rate sensors have been integrated to get the breadboard's orientation. This is then compared with the orientation of the end effector. The whole experiment (approx. 17 min) has been split into 8 partitions to not have the error grow out of bound. For each of the partitions the ARW has been determined. Figure 10 shows the error of one selected partition. The peaks come from a time shift between robot data and IMU data. The maximum ARW resulting from this test is 55.53°/sqrt(h). The high error terms are most likely coming from the commercial gyros. Their biases have changed since calibration two weeks earlier. It will be shown later that, by the use of a Kalman Filter, the estimation with the commercial gyros can be improved.

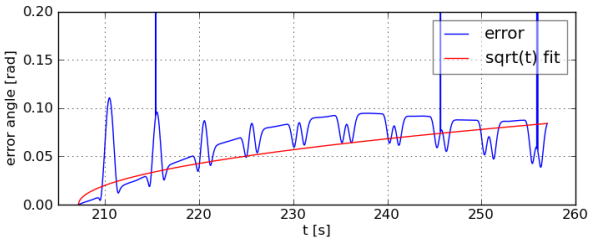

Figure 10. Orientation error for test on robotic arm.

Due to its very own dynamics the DFKI's Asguard system delivers very noisy data. It is possible to estimate the heading with only the SEA gyro (see Figure 11). But the data shows that more processing is necessary for such a system to improve the estimate since the ARW is approx. 93°/sqrt(h).

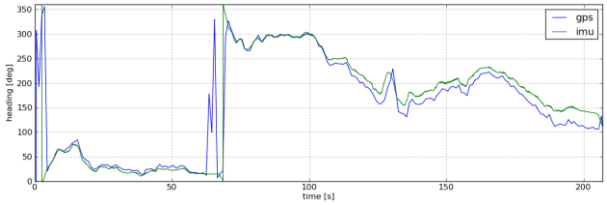

Figure 11. Heading estimate on the Asguard system.

A far better result can be estimated for a typical exploration rover like the LRM rover available at ESTEC. One experiment done in the ESTEC testbed was a 180° Ackerman circle fore and back with a speed of 2 cm/s. The heading error when summing up the rate signal from the space rate sensor is depicted in Figure 12. Fitting curves to the error curve gives the 3.1°/h for the linear fit and 0.83°/sqrt(h) for the square root fit. It shows a small error compared to the test with the Asguard system, although it is still bigger than required for the missions.

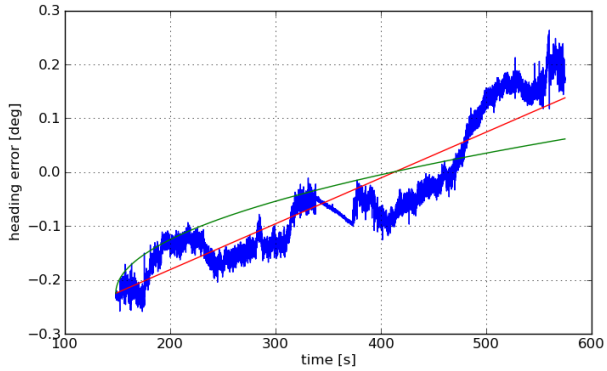

Figure 12. Error in heading estimate during the Ackerman maneuver with linear fit (red) and square root fit (green).

To improve the estimation of the orientation the information on the orientation from the integration and from the gravity measurement of the accelerometer can be combined with a Kalman Filter. The result of such a filtering can be seen in Figure 13. It shows the error between the orientation estimation of the IMU and the end effector orientation for the robotic arm test mentioned in the beginning of the section (IMU put into a wide range of orientations). This time it is not segmented and the integration error is steadily increasing. The second error line at the bottom of the graph shows the error after using the filter. There is no longer a tendency to grow but it remains stationary below an upper limit.

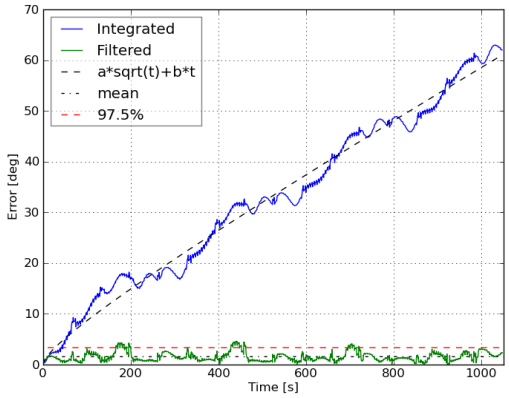

Figure 13. Error of integration and filtering.

Table 8 shows the error properties without and with Kalman filtering. The use of a filter can improve the orientation estimation such that the error is below 3.35° for 97.5% of the time. Replacing the two commercial sensors with the SEA gyro type will further improve the orientation estimation.

Table 8. Error properties for robotic arm test.

Integration Error	a=24.75 °/sqrt(h); b=163.94°/h
Mean Filter Error	1.56 °
97.5 % Filter Error	3.35 °

Further tests show the switch-off/switch-on behaviour of the IMU and the temperature stability. For all important sensors (SEA gyro and accelerometers) the results lie within the expected values. Apart from this activity the SEA gyro has recently been demonstrated on the CryoSat 2 satellite [10]. After 150 days of measurements and correlation with the reference sensors on the spacecraft the unit has demonstrated the predicted performance levels.

6 CONCLUSION AND OUTLOOK

This paper illustrates as a result of the Phase I ESA study that a complete IMU including post-filtering could be developed today using existing packaging techniques and available components in naked form with a maximum weight of ~250g and a volume of 500cm^3. The targeted accuracy can be achieved with improved sensors and data processing. The miniaturisation is possible by using the right combination of materials.

Nevertheless further work is necessary to enable a final miniaturized IMU. This includes using SEA Harmonised Gyro and equivalent accelerometers for all three axes, modifying the MRS Gyro circuit design to suit maximum use of bare die, a new PSU to minimise both power loss and physical size, modification of the current FPGA code to allow 'flash-based' FPGAs as bare die to be used and also enable in-flight re-programmability and refining the test, analysis and processing methods to achieve the best possible accuracy. After this, a prototype miniaturised IMU package with the full required performance could be demonstrated.

Furthermore, the study points out schemes for useful application of miniaturised IMUs based on high-performance MEMS sensors. For instance, the IMU can support rover navigation in combination with odometry, SLAM or other sensor suits. Here, the IMU provides resource-lean data that can off-load processing-intensive tasks. Also, the IMU seems particularly well suited for rapid traverse navigation, in future long-range rover missions.

REFERENCES

1. TEC-MMA/2008/72, Statement of Work - Multi Wafer Hybrid Integration: Rover IMU
2. P5-5-10-SR-039 Summary report - Multi Wafer Hybrid Integration Rover IMU 1
3. NEXT-LL-PDD-ESA(HME)-0001, Next-Lunar-Lander With In-Situ Science and Mobility: Phase A Mission Study Science and Payload Definition Document
4. NASA 431 RQMT-000045 Rev. B,Lunar Reconnaissance Orbiter Project - Radiation Requirements
5. D. W. Allan, "Statistics of atomic frequency standards," Proceedings of the IEEE, vol. 54, no. 2, pp. 221–230, 2005.
6. J. Hidalgo, P. Poulakis, J. Kohler, A. Barrientos, and J. Del-Cerro, "ESTEC Testbed Capabilities for the Performance Characterization of Planetary Rover Localization Sensors - First Results on IMU Investigations," presented at the *11th Symposium on Advanced Space Technologies in Robotics and Automation*, 2011.
7. IEEE, "Recommended Practice for Inertial Sensor Test Equipment, Instrumentation, Data Acquisition and Analysis," *IEEE Recommended Practice*, 2005.
8. IEEE, "Inertial Sensor Terminology," *IEEE Standard*, 2009.
9. S. Joyeux, J. Schwendner, F. Kirchner, A. Babu,, F. Grimminger, J. Machowinski, P. Paranhos, C. Gaudig, „Intelligent Mobility" in *KI - Künstliche Intelligenz*, Springer Berlin / Heidelberg, 2011
10. *ESA Press Release*: "Experimental MEMS sensor passes in-orbit test on CryoSat-2", 26 October 2010, *www.esa.int/esaLP/SEMM2AZOBFG_LPcryosat_0.html*